Differential Diffusion Effect in H2/NH3 Non-Premixed Flames and Flamelet-Based Models

Ahmed Adam
Interdisciplinary Graduate School of Engineering Sciences (IGSES), Kyushu University

Watanabe, Hiroaki
Interdisciplinary Graduate School of Engineering Sciences (IGSES), Kyushu University

https://doi.org/10.5109/7323262

出版情報：Proceedings of International Exchange and Innovation Conference on Engineering & Sciences (IEICES). 10, pp.190-197, 2024-10-17. International Exchange and Innovation Conference on Engineering & Sciences
バージョン：

Differential Diffusion Effect in H_2/NH_3 Non-premixed Flames and Flamelet-Based Models

Ahmed Adam[1,2,*], Reo Kai[1], Hiroaki Watanabe[1]
[1]Interdisciplinary Graduate School of Engineering Sciences (IGSES), Kyushu University, Fukuoka, Japan, [2]Mechanical Power Engineering Department, Faculty of Engineering, Helwan University, Cairo, Egypt
*Corresponding author E-Mail: Adam.ahmed.542@s.kyushu-u.ac.jp

Abstract: *The primary focus of this work is to examine the differential diffusion effect for flames fueled by H_2/NH_3. For a non-premixed turbulent flame, two Direct Numerical Simulations (DNS) have been implemented in two-dimensional domain, one is considering the differential diffusion (DD) of each species pair and the other assumes Unity Lewis Number (ULN). Two Flamelet libraries are created based on ULN and Mixture Averaged Diffusion (MAD) assumptions, they are validated through priori tests based on the DNS results. Significant difference between the two DNS cases, the DD case is more resistible for quenching than ULN case, meaning ULN assumption for DNS is not suitable. Furthermore, significant variations in the chemistry states are also evident in ULN library results, suggesting that differential diffusion should be considered in the Flamelet model, additionally, equal diffusivities is inappropriate for an H_2/NH_3-fueled flame, while MAD library exhibits more consistent chemistry states with the DD DNS.*

Keywords: Differential diffusion, Ammonia, Hydrogen, Flamelet progress variable model

1 INTRODUCTION

For the foreseeable future, burning fossil fuels and renewable energy sources will likely continue to be the primary methods of energy production. This reliance is central to the climate change conversation because it significantly contributes to greenhouse gas emissions. Hydrogen is considered a viable alternative for achieving a zero-carbon-emission society, but significant advancements are still needed for its large-scale storage and transportation.

In this context, ammonia has garnered significant attention due to its advantageous chemical properties and substantial economic potential. It has a low condensation pressure, a relatively high boiling point, and a higher volumetric energy density (MJ/L) compared to liquid hydrogen and batteries, making it suitable for energy storage and transport [1]. Established methods for ammonia production, storage, and transportation can be utilized without significant new investments, and its potential applications are enhanced by its flexibility and versatility [2].

The International Energy Association ranks ammonia among the most attractive fuels, a view supported by Japanese energy organizations, which list it as one of the top three promising energy carriers. However, ammonia's low flammability presents challenges for combustion, on the other hand, one possible solution is blending ammonia with hydrogen, because it enhances flame stability while maintaining carbon-free combustion. Additionally, the hydrogen required for cofiring can be produced locally using a catalyst to decompose ammonia into hydrogen and nitrogen, yielding a 3:1 volume ratio of hydrogen X_{H_2} to nitrogen X_{N_2}. Furthermore, cofiring is considered one of the ways to enhance the combustion characteristics of low grade fuels or fuel with low reactivity [3-5].

The Hydrogen (H_2) combustion as a renewable fuel for achieving zero carbon emissions in engines [6]. Effective modeling of H_2 combustion requires understanding differential diffusion (DD) due to hydrogen's high diffusivity. Unlike hydrocarbon fuels, DD effects cannot be ignored in hydrogen combustion. This study simulates turbulent hydrogen jet flames, with and without DD, and compares them with laminar Flamelet solutions. It examines the suitability of classical and Bigler's mixture fraction Z and Z_{Bilger} for non-premixed turbulent combustion modeling. Results show that Z_{Bilger} better captures DD effects and mitigates tangential diffusion (TD). DD influences flame through thermal, chemical, and transport effects. Despite suppressed transport effects, significant chemical and thermal effects of DD persist, indicating the conventional DD parameter may not fully characterize DD effects in turbulent non-premixed flames.

Although ammonia oxidation chemistry is complex, DNS is a powerful tool for understanding ammonia-based flames. However, due to the complexity of combustion processes, these simulations can be expensive to run. **F**lamelet/**P**rogress **V**ariable (**FPV**) models offer a solution by handling complex mechanisms with reasonable computational costs. Instead of directly modeling the unclosed chemical source terms and solving transport equations for each species in a typical chemical mechanism, the FPV model uses an indirect mapping approach. This approach maps all complex chemical processes to a simplified system of tracking scalars, reducing it to just two key variables: a progress variable, which measures the global extent of the local mixture's reaction, and the mixture fraction, which tracks the mixing of fuel and oxidizer [7]. Therefore, the scalars must be tabulated based on the mixture fraction and progress variable to form a Flamelet library. This library is then used during the FPV approach simulations.

However, the Flamelet equations make certain assumptions regarding the diffusivities of reacting species. One common assumption is the **U**nity **L**ewis **N**umber (**ULN**), which implies that all species' diffusivities are equal to the thermal diffusivity. Another assumption is a **M**ixture **A**veraged **D**iffusion (**MAD**) for each species, indicating that the diffusivity of each species into all others is averaged into only one value. These assumptions overlook the detailed binary diffusion

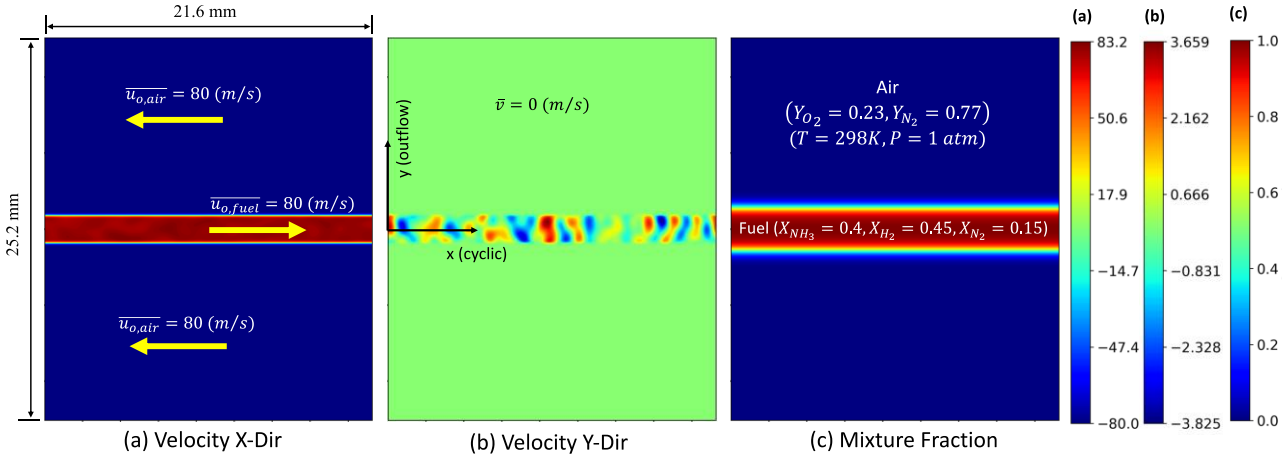

Figure 1 Initial distribution of the velocity's components (a & b) and the mixture fraction (c)

between individual species pairs. This oversight may be particularly problematic in the presence of hydrogen, which has a high diffusivity and significantly alters the diffusion behavior of all species in the flow field. Therefore, understanding the effect of differential diffusion in Flamelet-based models is essential.

This study aims to investigate the differential diffusion (DD) effect by conducting two Direct Numerical Simulations (DNS). One simulation considers DD, while the other assumes unity Lewis number (ULN), which is valid for most hydrocarbons due to their diffusivities being close to thermal diffusivity, though this is not the case for hydrogen. Furthermore, the DNS results are compared with predictions from Flamelet models based on ULN and MAD assumptions to evaluate the suitability of these assumptions in Flamelet-based approaches. Additionally, this study investigates the effect of the mixture fraction definition on estimating the location of the flame front.

2 NUMERICAL SETUP

2.1 Solved Equations

In this work, two DNS cases have been computed. The **D**ifferential **D**iffusion (**DD**) case solves the transport equations (1–4, 9), as well as the Stefan-Maxwell equation (6), which considers the binary diffusion for each species pair [8]. On the other hand, the ULN case solves the transport equations (1, 2, 7, 8, 9). Both cases solve the ideal gas equation of state (5).

In equations (1-9), the subscripts i and j denote spatial directions, while k and l indicate species. The variables are defined as follows: u represents bulk velocity, ρ is density, x denotes spatial distance, τ is shear stress, h stands for enthalpy, P represents pressure, Y is species mass fraction, X is species mole fraction, $\dot{\omega}_k$ is the net production rate of species k, V represents diffusion velocity, Ns is the number of species, Z is the mixture fraction, and α_{th} is thermal diffusivity.

The basic governing equations solved are the conservation of mass, momentum, energy, and mass fractions of chemical species.

In addition, a transport equation for the mixture fraction (Z) is solved, with the Lewis number set to unity [9], as shown in equation (9). The progress variable (C) is computed by summing the mass fractions of H_2 and H_2O. Based on Z and C from the DNS, the chemistry states in the Flamelet library with ULN or MAD can be mapped.

$$\frac{\partial \rho}{\partial t} + \frac{\partial \rho u_i}{\partial x_i} = 0 \tag{1}$$

$$\frac{\partial \rho u_i}{\partial t} + \frac{\partial \rho u_i u_j}{\partial x_j} = -\frac{\partial P}{\partial x_i} + \frac{\partial}{\partial x_j}\tau_{ij} \tag{2}$$

$$\frac{\partial \rho h}{\partial t} + \frac{\partial \rho u_i h}{\partial x_i} = \frac{\partial P}{\partial t} + u_i \frac{\partial P}{\partial x_i} + \frac{\partial}{\partial x_i}\left[\rho \alpha_{th}\left(\frac{\partial h}{\partial x_i} - \sum_k \left(h_k \frac{\partial Y_k}{\partial x_i}\right)\right) - \rho \sum_k \left(h_k Y_k V_{k,i}\right)\right] + \tau_{ij}\frac{\partial u_i}{\partial x_j} \tag{3}$$

$$\frac{\partial \rho Y_k}{\partial t} + \frac{\partial \rho u_i Y_k}{\partial x_i} = -\frac{\partial}{\partial x_i}\left(\rho V_{k,i} Y_k\right) + \rho \dot{\omega}_k \tag{4}$$

$$P = \rho R T \tag{5}$$

$$\frac{\partial X_k}{\partial x_i} = \sum_{l=1}^{Ns}\left(\frac{X_k X_l}{D_{k,l}}\right)(V_l - V_k) \tag{6}$$

$$\frac{\partial \rho h}{\partial t} + \frac{\partial \rho u_i h}{\partial x_i} = \frac{\partial P}{\partial t} + u_i \frac{\partial P}{\partial x_i} + \frac{\partial}{\partial x_i}\left(\rho \alpha_{th}\frac{\partial h}{\partial x_i}\right) + \tau_{ij}\frac{\partial u_i}{\partial x_j} \tag{7}$$

$$\frac{\partial \rho Y_k}{\partial t} + \frac{\partial \rho u_i Y_k}{\partial x_i} = \frac{\partial}{\partial x_i}\left(\rho \alpha_{th}\frac{\partial Y_k}{\partial x_i}\right) + \rho \dot{\omega}_k \tag{8}$$

$$\frac{\partial \rho Z}{\partial t} + \frac{\partial \rho u_i Z}{\partial x_i} = \frac{\partial}{\partial x_i}\left(\rho \alpha_{th}\frac{\partial Z}{\partial x_i}\right) \tag{9}$$

2.2 Initial and boundary Conditions

A temporally evolving non-premixed planar turbulent jet flame is computed in the present DNSs. The configuration is equivalent to a square domain with a 2D isotropic turbulence field superimposed over a fuel stripe that is surrounded by air in two dimensions. An isotropic, homogeneous turbulent kinetic energy spectrum is used to initialize the turbulent field [8], [10]. In this spectrum, the integral length scale L_{11} is 0.6 mm, and the fuel core fluctuates at a rate of 8 m/s, as shown in Figure 1 (a) and (b).

Table 1 The investigation program

Case No.	Type	DNS's Diffusion Model	Flamelet Library's diffusion model	Mixture fraction used for mapping	Mixture fraction used to estimate flame front
1	DNS	DD	-	-	Z_{ULN}, Z_{Bilger}
2	DNS	ULN	-	-	Z_{ULN}, Z_{Bilger}
3	Mapped	-	ULN	Z_{ULN}	-
4	Mapped	-	ULN	Z_{Bilger}	-
5	Mapped	-	MAD	Z_{ULN}	-
6	Mapped	-	MAD	Z_{Bilger}	-

The initial fuel stripe thickness H_o is 1.8 mm, with mean velocity of 80 m/s while the surrounding air has the same mean velocity in the opposite direction; i.e., $\overline{u_{o,air}} = -\overline{u_{o,fuel}} = 80\ m/s$, the relative velocity $\Delta U_o = \overline{u_{o,air}} - \overline{u_{o,fuel}}$ =160 m/s.

The initial distribution of temperature and mass fractions is obtained from the MAD Flamelet library. By extracting the Flamelet solution of the highest scalar dissipation rate just before the extinction from the library, meaning that a solution with only one independent variable, the mixture fraction, is obtained.

This mixture fraction is then used to determine the rest of the scalar values. Therefore, once the mixture fraction distribution is initialized, the remaining scalar values can be derived. The mixture fraction is initialized as shown in Figure 1 (c).

The computational domain consists of uniform grid points measuring 25 µm in size, with 1008 horizontal and 864 vertical grid points.

Furthermore, as shown in Figure 1, the distribution of velocity and mixture fraction exhibits a gradual transition from the fuel side to the air side. This smooth transition is crucial for numerical stability and convergence, achieved by using the tanh hyperbolic function to ensure a smooth distribution of the mixture fraction and the rest of the scalars. This overall initialization is obtained from Hawks et al. [11].

2.3 Fuel Composition

The fuel stream is composed of NH_3, H_2, and N_2 with respective volume fractions of 40%, 45%, and 15%. This composition results from mixing two streams: the first stream contains 57% of the main ammonia stream, while the second stream consists of the remaining 43% of the main ammonia, decomposed into hydrogen and nitrogen.

2.4 The FK^3 solver

FK^3 is an in-lab code used in DNS [12]. This code utilizes the fractional-step algorithm to implement a pressure-based semi-implicit solver. To preserve accuracy, spatial derivatives for convection terms in the momentum equation are estimated using a fourth-order central difference scheme. Scalar calculations are performed using a fifth-order Weighted Essentially Non-Oscillatory (WENO5) scheme in the meantime. A second-order central difference scheme is used to discretize diffusive terms and a fourth-order central difference scheme is used to evaluate the spatial derivatives of the stress tensor. The third-order explicit TVD (Total Variation Diminishing) Runge-Kutta method is used for time integration for convection terms. The Variable-coefficient Ordinary Differential Equation (VODE) approach is used to compute the ordinary differential equations for the detailed chemistry mechanism.

$$Z = \frac{\frac{Z_C}{\nu_C W_C} + \frac{Z_H}{\nu_H W_H} + 2\frac{(Z_{O,2} - Z_O)}{\nu_O W_O}}{\frac{Z_{C,1}}{\nu_C W_C} + \frac{Z_{H,1}}{\nu_H W_H} + 2\frac{Z_{O,2}}{\nu_O W_O}} \tag{10}$$

2.5 Mixture Fraction Definitions

The mixture fraction used in this study is defined in two ways. The first is the transport equation based on the ULN assumption, see equation (9). The second uses Bilger's definition, see equation (10) [9], where Z_C, Z_H,

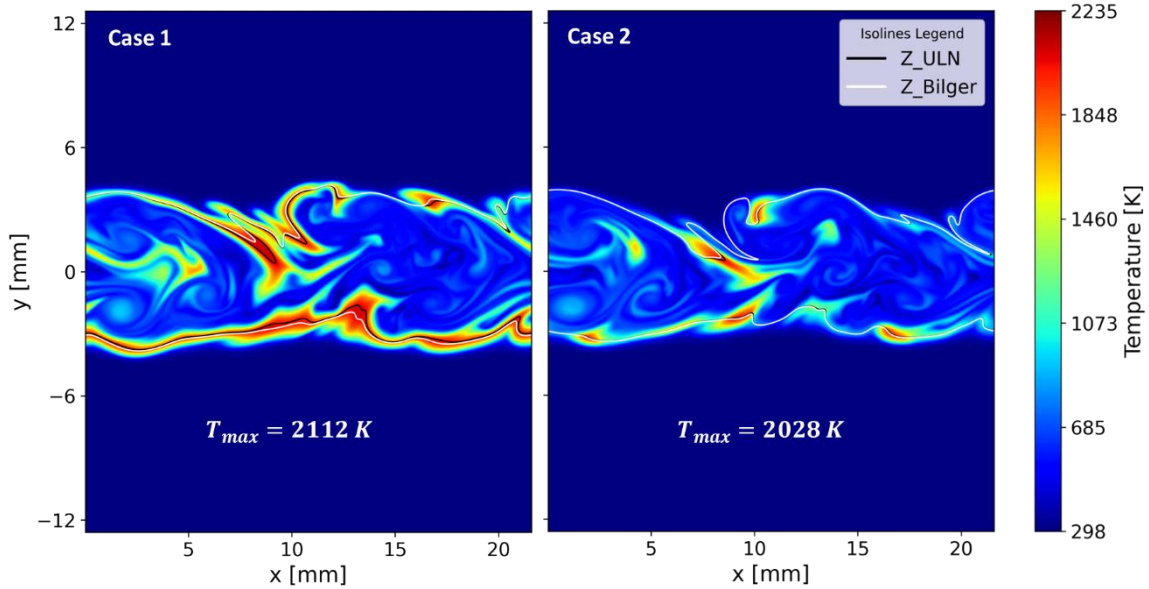

Figure 2 Temperature contours for cases 1 (left) and 2 (right). The isolines represent stoichiometric mixture fraction, white for Bilger's definition and black for ULN definition.

and Z_O are the elemental mass fractions of carbon, hydrogen, and oxygen, respectively. Furthermore, 1 and 2 represent fuel and air streams respectively.

3 RESULTS AND DISCUSSION

This section is divided into two main parts, the first part (3.1, 3.2 and 3.3) is to investigate the results of DNS cases 1 and 2. The second part (3.4) tests the Flamelet libraries by comparing their mapped results (cases 3-6), with the DNS case number 1, as explained in Table 1. All the data shown in this section are obtained at a time equal to 22.2 of the reference time $t_{ref} = H_O/\Delta U_O$, at which the turbulence field is completely independent of the initial one.

3.1 Flame Front Location

The flame front location is in the vicinity of the stoichiometric mixture fraction, so it is reasonable to approximate its location to be at Z_{st}. According to the two definitions used in this study, the mixture fraction fields differ for the same case. Although the contours of the mixture fraction based on these two definitions are nearly identical, some differences appear at mixture fraction values near the stoichiometric one, as shown in Figure 2 for both case 1 (DD DNS case) and case 2 (ULN DNS case), especially at high-temperature regions.

The deviation is strong in case 1 where the Fickian diffusion is considered, while it's weak in case 2 where ULN is assumed. However, it's notable that at high-temperature regions the deviation notably increases in the case 2 as well.

To investigate the flame front location more accurately, the temperature maxima distribution could be used for this purpose as shown in Figure 3. In case 1, the distribution differs significantly based on the way of defining the mixture fraction unlike case 2, as it's also observed in Figure 2. Nevertheless, regarding case 1, Figure 3 shows that the highest maximum based on Z_{Bilger} is located just on the right to the stoichiometric mixture fraction, meaning it is located in the slightly fuel-rich zone, unlike the maximum based on Z_{ULN} which is in the fuel-lean zone. Based on this, the location of the flame front is estimated more precisely using Bilger's equation (10) as such distribution is commonly observed in the literature, see [13] Chapter 1.

Furthermore, regarding case 2, Figure 3 shows a slight difference between the maxima distribution in the fuel-lean zone and the slightly fuel-rich zone. The maximum temperature is also located in the slightly fuel-rich zone based on Z_{Bilger} , while it is located at stoichiometric Z_{ULN}. This suggests that Z_{Bilger} might have an advantage over Z_{ULN}, even in a full DNS simulation based on the ULN assumption to estimate the from front location, as in case 2.

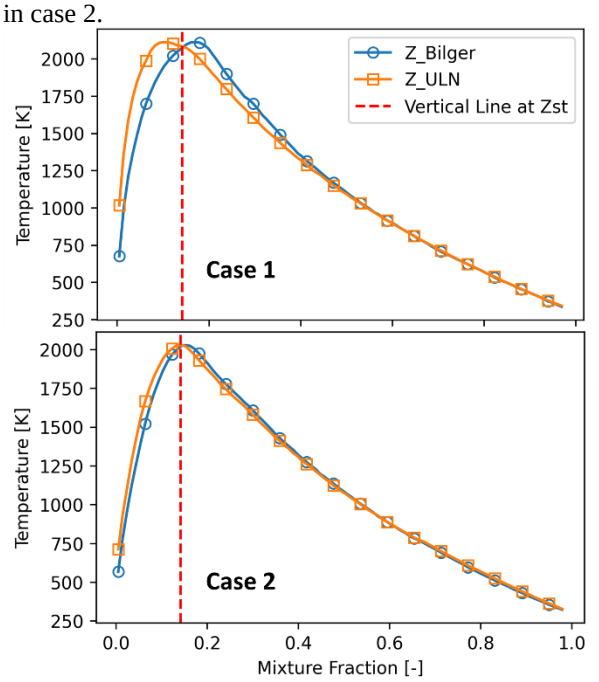

Figure 3 Temperature maxima distribution in mixture fraction space, case 1 above, case 2 below, with marker interval = 6 for both

3.2 Momentum Effect of DD

The DD has a notable effect on the velocity magnitudes and directions, as shown by the contours of velocity magnitude and streamlines in Figure 4. Cases 1 and 2 exhibit clear differences, indicating the impact of DD. The DD effect continually changes the momentum of each individual species, eventually altering the distribution of all species' mass fractions and the flow velocity components.

Despite the momentum equation (2) not containing a term for diffusion velocities, DD affects it by changing

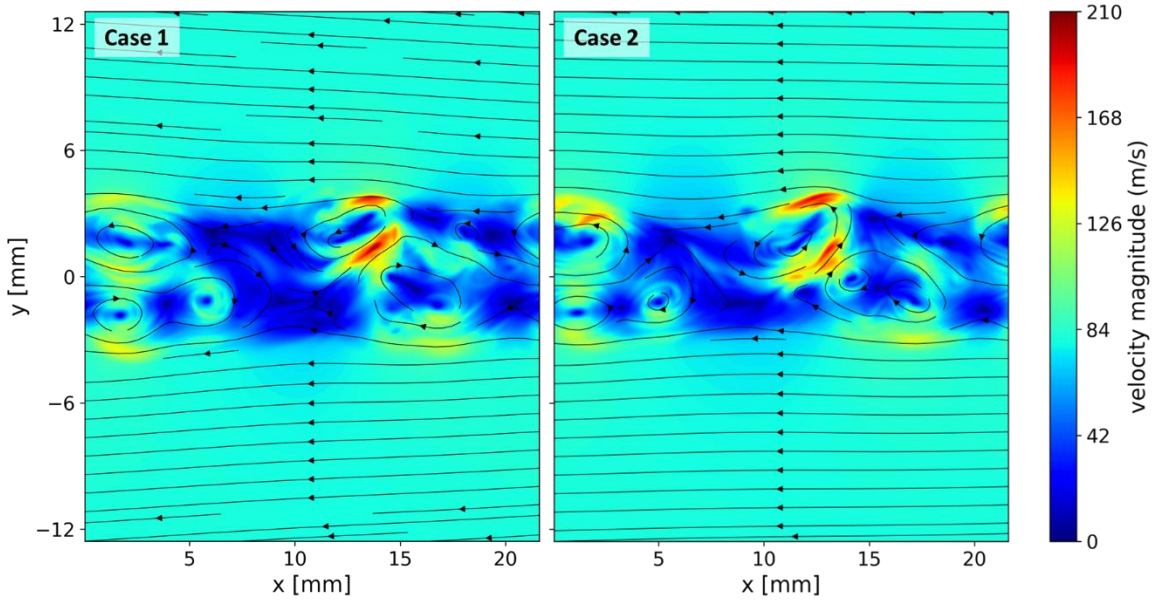

Figure 4 Velocity magnitude contours with streamlines for case 1 (left) and case 2 (right)

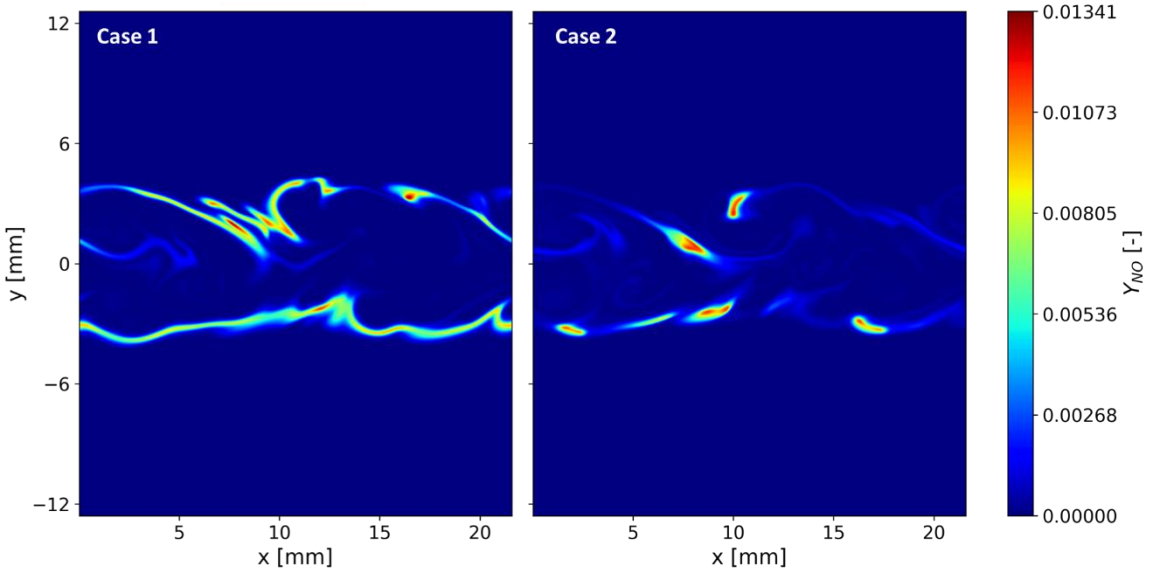

Figure 6 Distribution contours of the nitrogen oxide mass fractions. Case 1 (left) and case 2 (right)

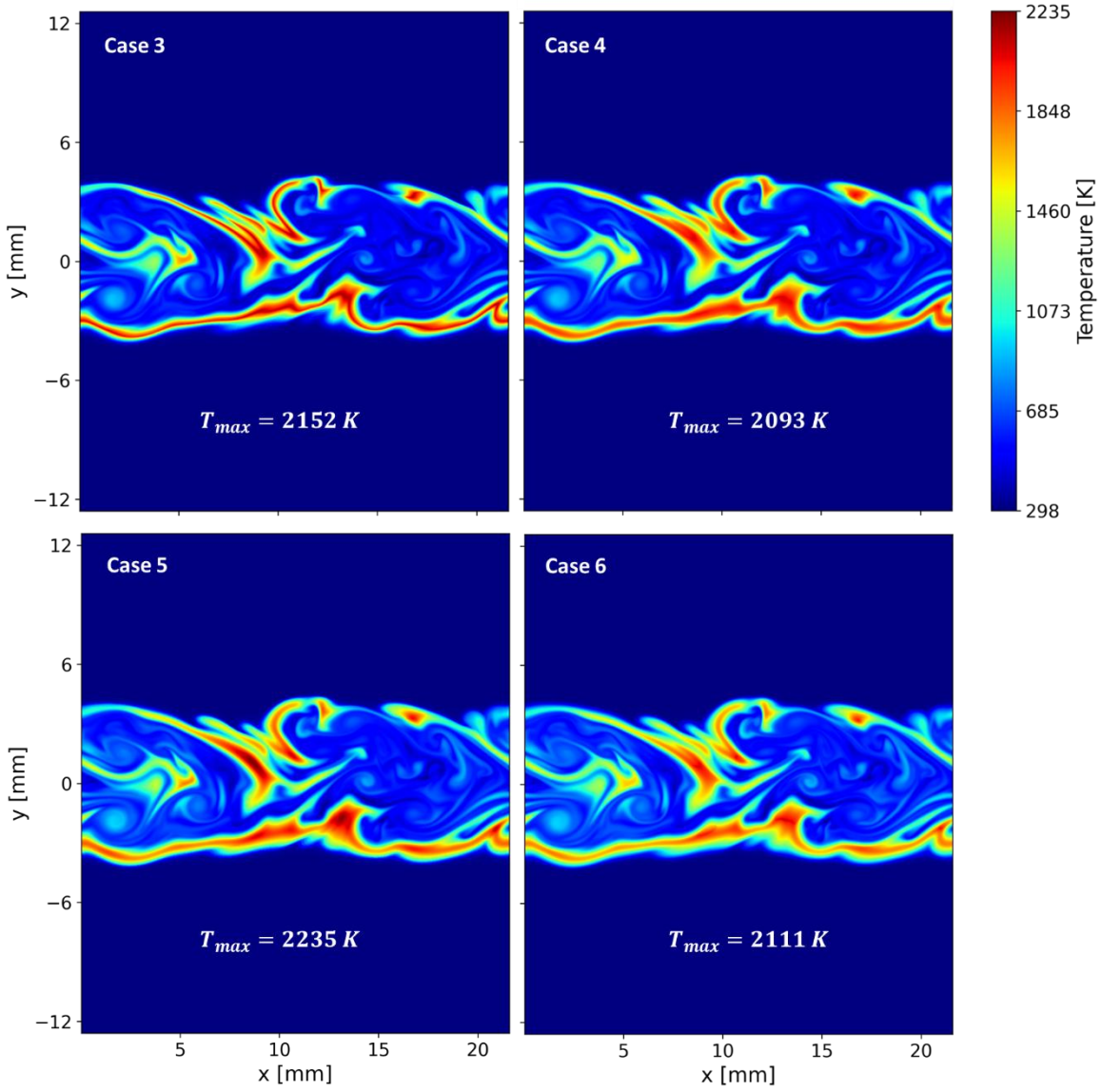

Figure 5 Temperature contours for the mapped Flamelet libraries, based on Case 1's Z and C

the density of the mixture, which in turn changes the velocities. Therefore, the momentum is indirectly influenced by DD. Furthermore, this mechanism is also present when considering ULN, but it is evident that DD has more influence on the momentum than ULN.

The chemical effect [6] contributes to the momentum effect, as the diffusion of hydrogen and ammonia toward the flame front increases the reaction rates in case 1 more than in case 2. This results in an increase in product species and a decrease in reactant species, changing the

local density of the mixture in and around the flame front and subsequently affecting the momentum of the flow in this area.

3.3 Scalars Distribution in DNS Cases

As shown in Figure 2, the isolines represent flame fronts for the same definition in case 1 and case 2 are not identical, despite having identical initial and boundary conditions. This indicates that the DD has a notable effect on the mass fractions distribution throughout the entire domain, especially near the reaction zone.

The temperature distribution differs between case 1 and case 2. The temperature is higher in case 1, indicating that high hydrogen diffusivity enhances the overall diffusion process, resulting in more fuel diffusing toward the reaction zone. This sustains high reaction rates and keeps the flame ignited. In contrast, in case 2, the suppressed hydrogen diffusion leads to quenched flames in many zones, as shown in Figure 2.

Furthermore, the different temperature distributions between case 1 and case 2 lead to different density distributions, which strengthen the momentum effect of the DD and the thermal expansion in case 1 due to the higher temperature.

In addition, the mass fraction distribution of nitrogen oxides is underestimated in case 2 due to the lower temperature and reaction rates, as shown in Figure 6. This is significant because nitrogen oxides are one of the most unwanted products of ammonia combustion.

Based on the temperature and nitrogen oxides distribution, the heat release rate is also underestimated in case 2. This indicates that the ULN assumption is not suitable for simulating NH_3/H_2 combustion.

3.4 Flamelet Libraries Priori Tests

The importance of the FPV approach lies in its ability to reduce computational cost. Instead of solving the energy and mass fraction transport equations during the computation, the Flamelet equations which are conservation equations of energy and mass species are solved prior to the computation to obtain the scalars such as temperature, mass fractions, enthalpy and many other. Then the Flamelet solutions are organized into a library, conditioned on the mixture fraction and progress variable. After that, during the CFD simulation, in addition to the continuity and momentum transport equations, transport equations, for Z and C, need to be solved instead of the energy and mass fraction equations. The results of Z and C serve as inputs to the Flamelet library to retrieve the rest of the necessary data.

In this study, the FPV approach is not used in the computations; instead, DNS is used for cases 1 and 2. The case 3 to 6 are mapped cases using the Flamelet libraries based on the results of the DNS (priori tests).

Two Flamelet libraries are investigated by comparing their mapped results with a single DNS. In case 1, one library is generated based on the unity Lewis number (ULN), and the other is based on the Mixture Averaged Diffusion (MAD). This approach is used to investigate the effects of all possible assumptions related to the diffusion process made in Flamelet solutions. Both libraries are obtained through the open source FlameMaster software [14]. The ULN Flamelets are solved in the mixture fraction space, while the MAD equations are solved in physical space. Then both libraries are generated in the mixture fraction space based on the solutions of the Flamelets for both cases.

The MAD assumption is generally closer to DD than ULN. While ULN assumes that all diffusion coefficients are equal and to the thermal diffusivity, MAD does not make this assumption. Instead, MAD assumes that each species has an average diffusion coefficient for diffusing through the rest of the species in the mixture. Consequently, MAD does not consider binary diffusion between each species pair. However, it is more consistent with DD because it accounts for each species having a

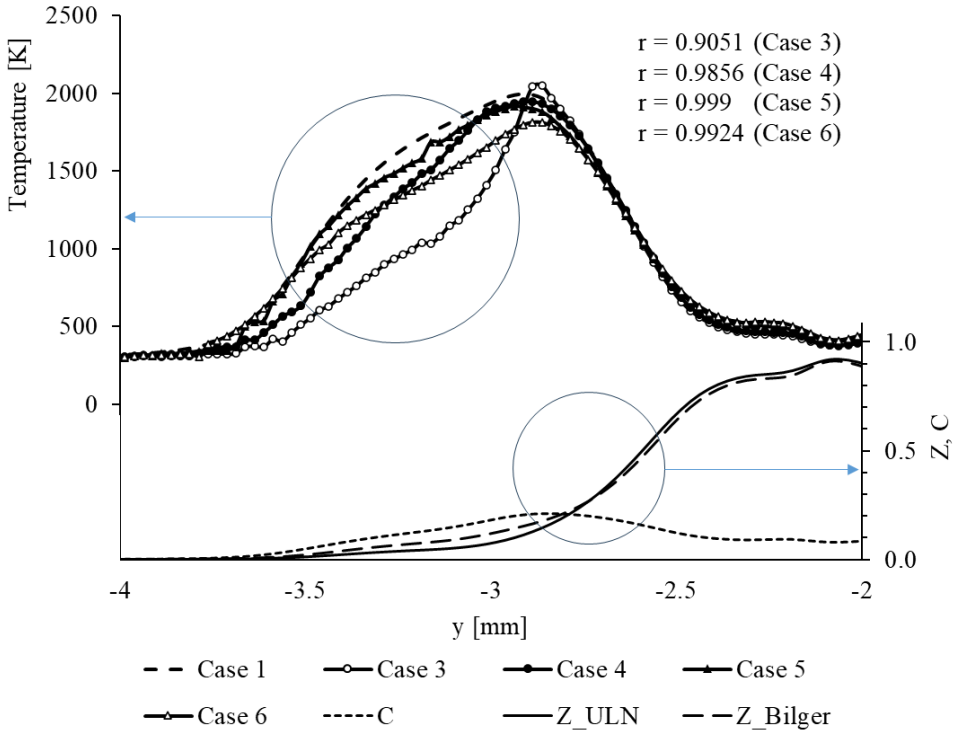

Figure 7 Temperature distributions at a vertical line (x=8 mm) along with the mixture fraction (Z) and progress variable (C) distributions

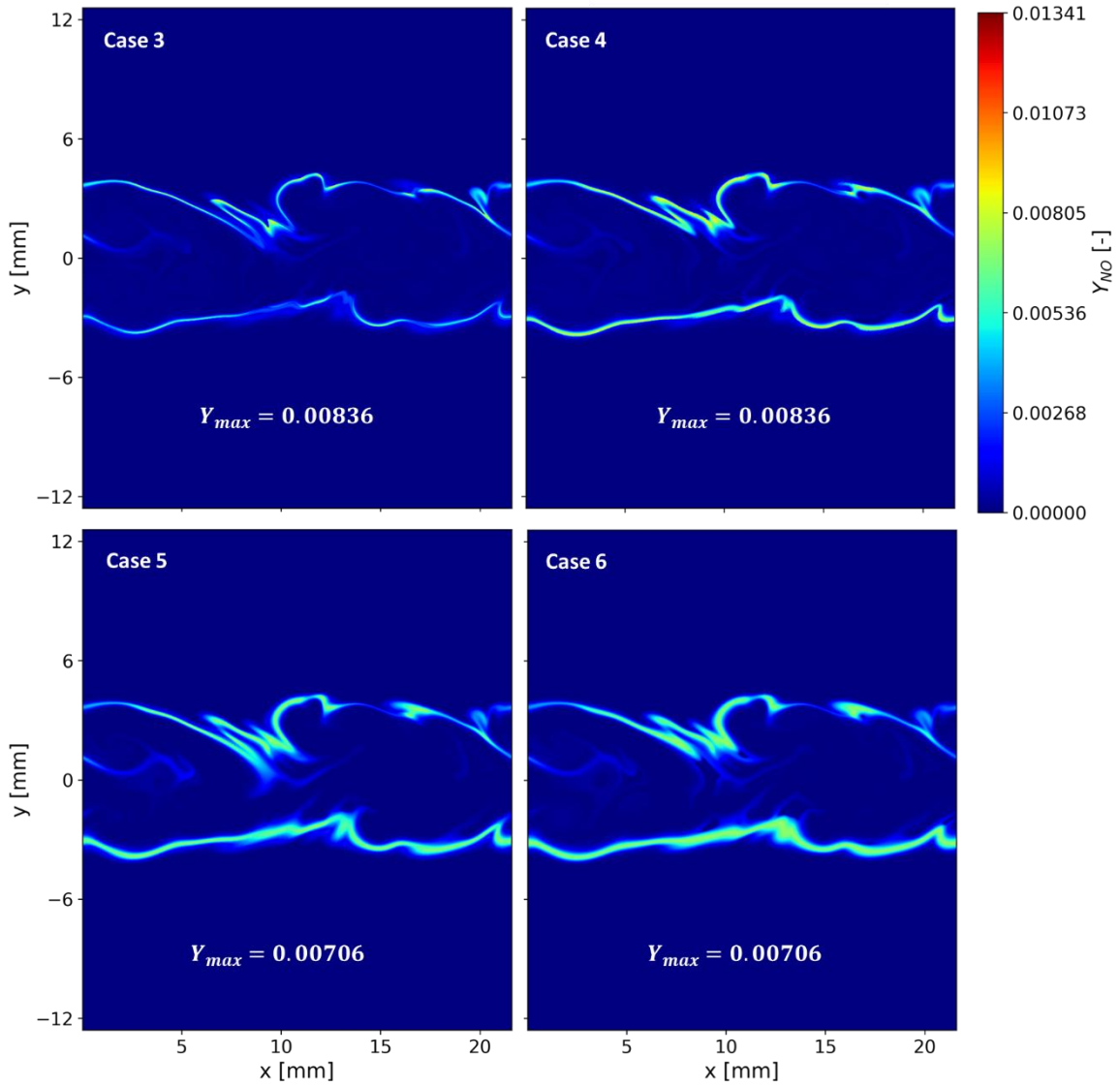

Figure 8 Y_{NO} distribution for the mapped cases

different diffusivity, which is calculated based on the mass fractions of rest of species locally at each grid point. Figure 5 shows the temperature contours of the mapped Flamelet libraries over the case 1 mixture fraction and progress variable ($C = Y_{H_2O} + Y_{H_2}$), the mapped temperature distributions are nearly the same, however, some crucial differences still exist. The maximum temperature distributions are not compatible with the case 1, especially in cases 3 and 5 where ULN mixture fraction (9) are used, while Bilger's mixture fraction showed more smooth temperature distributions while keeping narrow zones with higher temperatures than case 1. Furthermore, the values of the maximum temperatures deviated as well in the mapped cases from the Case 1, therefore, to quantitatively investigate the distribution of the temperature, its values are extracted at a vertical line in the domain ($x = 8$ mm) then plotted as shown in Figure 7.

The mapped results from the ULN library using Z_{ULN}, case 3, showed the lowest correlation factor (r) with case 1. This is expected as both the library and mixture fractions do not consider the differential diffusion. However, the mapped result from the ULN library using Z_{Bilger} showed a significant improvement, which could be attributed to the ability of the Z_{Bilger} to estimate the flame front location more accurately.

On the other hand, the mapped results from the MAD library showed better agreement with the DNS than ULN library by using both Z_{Bilger} and Z_{ULN} as expected. Case 5 showed the highest correlation factor with case 1 followed by case 6. Which gives an advantage for using MAD library with Z_{ULN} to be used in FPV approach for NH_3/H_2 combustion. Furthermore, Z_{ULN} unexpectedly showed better performance than Z_{Bilger} in mapping results from MAD library regarding the correlation factor, while the Z_{Bilger} estimated the maximum temperature more accurately as in Figure 5.

Nevertheless, the mapped results from both libraries could exceed the DNS temperature near the reaction zone especially when Z_{ULN} is used for mapping. Which requires a careful library generation by increasing its resolution near the Z_{st} and smoothing the distribution inside it as possible. If a good library is generated it will not be flawless, however, by taking the average during a simulation using FPV approach helps to enhance the results accuracy.

Furthermore, both libraries underestimated Y_{NO} as shown in Figure 8, which is one of the drawbacks of FPV approach, however a correction method is developed by [15] to more accurately estimate Y_{NO} by solving the Y_{NO} transport equation while using the library to calculate the source term.

4 Conclusion

This study aims to investigate the differential diffusion effect in NH_3/H_2 combustion in DNS and FPV simulations as well. Only DNS are implemented, while the Flamelet based libraries are investigated using priori tests. FK^3 solver is used to implement the DNS cases and FlameMaster software is used to generate the Flamelet libraries based on ULN and MAD assumption for diffusion. The main findings are as follow:

- The Bilger's definition of the mixture fraction more accurately estimate the flame front location in NH_3/H_2 differential diffusion combustion simulations than the transport equation definition with ULN assumption.
- The differential diffusion alters the local density and the distribution of the mass fractions through its transport, thermal and chemical effects, which eventually alters the momentum of the main flow. This is described as momentum effect.
- The mapped temperature from the Flamelet library generated with the ULN showed huge deviation from the DNS results, however, its mapped temperature by Z_{Bilger} showed a significant improvement. While the mapped temperature from the MAD library showed good agreement with the DNS results, especially when Z_{ULN} is used.
- Both Z_{ULN} and Z_{Bilger} have pros and cons when they are used to map the MAD Flamelet libraries, which opens the door for future work to investigate the way of mapping the library using both mixture fraction definition to take the advantage of each one.
- The effect of the mixture fraction definition, used to condition the data within the Flamelet library, was not included in this study, indicating an area for future investigation.

Those findings showed that differential diffusion must be taken into consideration while studying the NH_3/H_2 through a numerical approach, as DD has great effects on the thermo-chemical state of the flame in addition to the flow field as well.

5 Acknowledgements

This work is partially supported by MEXT as "Program for Promoting Researches on the Supper-computer Fugaku" (Smart Design Realized on the Supercomputer "Fugaku" in the Society 5.0 Era) and used computational resources provided by the RIKEN Center for Computational Science (Project ID: hp220180, hp230193, hp240205).

6 REFERENCES

[1] H. Kobayashi, A. Hayakawa, K. D. K. A. Somarathne, and E. C. Okafor, "Science and technology of ammonia combustion," Proc. Combust. Inst., vol. 37, no. 1, pp. 109–133, 2019, doi: 10.1016/j.proci.2018.09.029.

[2] A. M. Elbaz, S. Wang, T. F. Guiberti, and W. L. Roberts, "Review on the recent advances on ammonia combustion from the fundamentals to the applications," Fuel Commun., vol. 10, no. February, p. 100053, 2022, doi: 10.1016/j.jfueco.2022.100053.

[3] A. A. Adam, M. A. Shahein, A. E. El-Kholy, and H. A. Moneib, "Cofiring of Oil and Gaseous Fuels Through an Innovative Coaxial, Double Swirl Burner," Int. Exch. Innov. Conf. Eng. Sci., vol. 9, pp. 79–85, 2023, doi: 10.5109/7157952.

[4] S. Yadav, P. Yu, K. Tanno, and H. Watanabe, "Large eddy simulation of coal-ammonia flames with varied ammonia injection locations using a flamelet-based approach," Energy, vol. 276, no. March, p. 127546, 2023, doi: 10.1016/j.energy.2023.127546.

[5] M. M. Salama, E. Elsihy, H. Moneib, M. Kamal, and M. Shahein, "The Combustion of a Diesel Oil-Based/Coal/Water Slurry in a Horizontal Cylindrical Furnace: An Experimental Investigation," Int. Exch. Innov. Conf. Eng. Sci., pp. 64–70, 2021, doi: 10.5109/4738568.

[6] W. Han, A. Scholtissek, F. Dietzsch, and C. Hasse, "Thermal and chemical effects of differential diffusion in turbulent non-premixed H2 flames," Proc. Combust. Inst., vol. 38, no. 2, pp. 2627–2634, 2021, doi: 10.1016/j.proci.2020.06.049.

[7] C. D. Pierce and P. Moin, "Progress-variable approach for large-eddy simulation of non-premixed turbulent combustion," J. Fluid Mech., vol. 504, no. March 2002, pp. 73–97, 2004, doi: 10.1017/S0022112004008213.

[8] H. Shehab, H. Watanabe, Y. Minamoto, R. Kurose, and T. Kitagawa, "Morphology and structure of spherically propagating premixed turbulent hydrogen - air flames," Combust. Flame, vol. 238, p. 111888, 2022, doi: 10.1016/j.combustflame.2021.111888.

[9] H. Pitsch and N. Peters, "A consistent flamelet formulation for non-premixed combustion considering differential diffusion effects," Combust. Flame, vol. 114, no. 1–2, pp. 26–40, 1998, doi: 10.1016/S0010-2180(97)00278-2.

[10] B. T. Passot and A. Pouquet, "Numerical simulation of compressible homogeneous flows in the turbulent regime," J. Fluid Mech., vol. 181, pp. 441–466, 1987.

[11] E. R. Hawkes, R. Sankaran, J. C. Sutherland, and J. H. Chen, "Scalar mixing in direct numerical simulations of temporally evolving plane jet flames with skeletal CO/H2 kinetics," Proc. Combust. Inst., vol. 31 I, no. 1, pp. 1633–1640, 2007, doi: 10.1016/j.proci.2006.08.079.

[12] R. Kurose, "About in-house code FK^3": http://www.tse.me.kyoto-u.ac.jp/study/link_e.php (accessed 22.10.7).

[13] C. K. Law, Combustion Physics. Cambridge University Press., 2006. doi: https://doi.org/10.1017/CBO9780511754517.

[14] H. Pitsch, "FlameMaster." Institute of Technical Combustion (itv). [Online]. Available: https://www.itv.rwth-aachen.de/downloads/flamemaster/

[15] M. Ihme and H. Pitsch, "Modeling of radiation and nitric oxide formation in turbulent nonpremixed flames using a flamelet/progress variable formulation," Phys. Fluids, vol. 20, no. 5, pp. 1–20, 2008, doi: 10.1063/1.2911047.